Optimal parameters of shock tubes to simulate the high explosive effect of a blast

Mikhail V. Chernyshov*, Karina E.* Savelova*, and *Anna A.* Yatsenko

Baltic State Technical University «VOENMEH», 190005 Saint-Petersburg, Russian Federation

Keywords: High explosive blast, Shock tube, Analytical shody, Shock-wave structures, Blast wave, Riemann expansion wave.

Abstract. The problem of generating pressure waves with a profile similar to the profile of a blast wave in closed shock tubes with constant cross-section is considered. Applying non-stationary gas dynamics methods, the dimensions (lengths) of high and low pressure chambers are determined analytically and numerically. Also, the gas parameters in those chambers necessary to produce pressure waves with a profile close to triangular are determined.

1 Introduction

For physical simulation of the high-explosive blast impact on a target (protected) object in Russia [1-4] and abroad [5-11], shock tubes are traditionally used. The advantages of this method of physical simulation over full-scale field tests are lower cost and easier reproducibility of the experiment, as well as its higher safety. At the same time, the question often arises about the physical adequacy of waves generated in shock tubes to blast waves generated in real conditions, which forces us to doubt on the reliability of laboratory results. A necessary condition for the adequacy of the experiment is the similarity of the pressure profiles of the shock waves created in shock tubes and the blast waves resulting at high-explosive detonation. In particular, a pressure wave, effect of which on an obstacle (the end of the shock tube) is studied experimentally, should have a static pressure profile close to triangular one, with a subsequent drop in pressure behind the wave to initial (atmospheric) value or lower (especially, if it is necessary to simulate not only the positive phase, but also the negative phase of the blast wave).

The problems of constructing shock tubes with a given pressure profile of the resulting waves were previously solved numerically and analytically [3, 12, 13]. The increased attention paid nowadays to testing various means of explosion protection makes it necessary to consider this issue in more detail. In particular, in this work, the minimal ratios of the sizes (lengths) of the high and low pressure chambers of the shock tube are determined, which make it possible to generate shock waves that have the required pressure profile at the moment of collision with the test object located at the end of the tube. In

* Corresponding author: karinkamurz@yandex.ru

addition, the degree of subsequent drop in static pressure in the co-current flow behind the positive phase has been determined, which allows us to achieve a more complete similarity of the shock waves in tubes and blast waves under consideration.

2 Brief description of the flowfield

The simplest shock tube with a constant cross-sectional area (Fig. 1a) consists of chambers of high (HPC) and low (LPC) initial pressures (p_{01} and p_{02}, respectively); here $p_{01}>p_{02}$. In the following, it is assumed that the chambers of the shock tube contain gas of the same chemical composition and temperature, that is, the adiabatic indices ($\gamma_1=\gamma_2=\gamma$) and the initial sound velocity ($a_{01}=a_{02}=a$) in the high-pressure section and the low-pressure one are equal. The initial state of the process is characterized by the pressure ratio $I = p_{01}/p_{02}$ before the rupture of the separating diaphragm O.

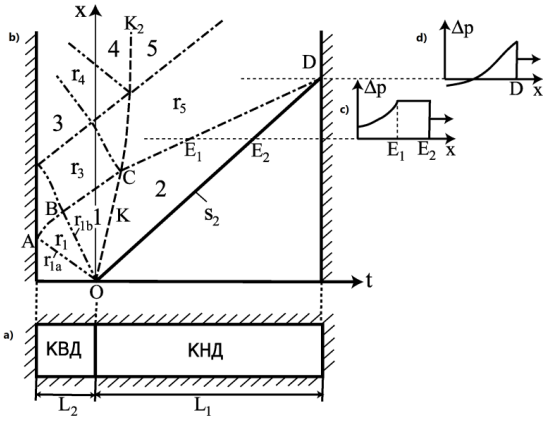

Fig. 1. Shock tube.

After the diaphragm ruptures, an isentropic centered Riemann rarefaction (expansion) wave r_1, a shock wave front s_2, and a contact discontinuity K form in the tube (Fig. 1b). The "left" isentropic expansion wave and the "right" shock one propagate, respectively, to the left and to the right relative to the gas particles, into the high and low pressure chambers, correspondingly. The contact discontinuity K serves as the interface between the gases originally located in those chambers. The expansion fan of the acoustical characteristics of the Riemann wave r_1 is limited by its leading (r_{1a}) and trailing (r_{1b}) fronts. Those border characteristics, at the same time, are the surfaces of so-called weak discontinuities. It means that the first derivatives of the flow parameters with respect to spatial coordinates and time (but not those parameters themselves) are discontinuous through those surfaces. When the "left" expansion wave r_1 reaches the solid wall (the left end of the shock tube), the "right" rarefaction wave r_3 reflects from it. The characteristics of the wave r_3 (in particular, its leading border BC) move at the local speed of sound relative to the gas particles and, therefore, overtake the contact discontinuity K. When the wave r_3 collides with the discontinuity K, a reflected Riemann wave (r_4) and another expansion Riemann wave passing through the discontinuity (r_5) appears, as well as a new contact discontinuity K_2, which has changed its speed compared to the previous one (K). Under conditions corresponding to the problem considered here ($a_{01}=a_{02}=a$, $\gamma_1=\gamma_2=\gamma$, $p_{01}>p_{02}$), wave r_4 compresses the flow (it is so-callled simple Riemann compression wave). The refracted rarefaction wave r_5 gradually overtakes the shock wave (s_2); in particular, it touches its leading edge CD is at point D. Gas flows in regions 1-5 behind shock and isentropic waves are uniform. Their gas-dynamic (p_i, a_i) and kinematic (i.e., the flow velocities) parameters

are determined by the strengths (intensities) J_i of waves s_i and r_i (i.e., the ratios of static pressures behind these waves and in front of them [2, 14]). According to the Rankine-Hugoniot and Laplace-Poisson adiabats, the ratio of the speeds of sound behind the shock wave (a_i) and in front of it (a_{i-1}) obeys as

$$a_i / a_{i-1} = \sqrt{J_i \left(1 + \varepsilon J_i\right) / \left(J_i + \varepsilon\right)} \; ; \tag{1}$$

Here $\varepsilon=(\gamma-1)/(\gamma+1)$. On the sides of the Riemann waves, sound velocityes obey as if follows :

$$a_i / a_{i-1} = J_i^{(\gamma-1)/2\gamma} \; . \tag{2}$$

The variation of the flow velocity $([u]_i=u_i-u_{i-1})$ is also determined by the intensity of the wave and the speed of sound in front of it:

$$\left[u\right]_i = \chi\left(1-\varepsilon\right)\widetilde{a}_i \cdot \left(\sqrt{\frac{J_i+\varepsilon}{1+\varepsilon}} - \sqrt{\frac{1+\varepsilon}{J_i+\varepsilon}} \right) \tag{3}$$

At the shock front (s_i), and

$$\left[u\right]_i = -\frac{2\chi\widetilde{a}_i}{\gamma-1} \cdot \left(1 - J_1^{(\gamma-1)/2\gamma}\right) \tag{4}$$

on an isentropic (r_i) Riemann wave. Here $\chi=1$ and $\chi=-1$ in the case of a “right” and “left” wave, respectively. The static pressures of the flows are related by the obvious relationship: $p_i=J_i \cdot p_{i-1}$. The conditions of equality of static pressures and gas flow velocities on both sides of the discontinuity K determine the wave intensities r_1 and s_2 from the system of equations

$$J_2 = IJ_1 \, , \; \left[u\right]_1 = \left[u\right]_2 \, ,$$

the solution of which is given in inverse form (shock tube equation):

$$I = J_2 \cdot \left[\frac{\sqrt{\left(1+\varepsilon\right)\left(J_2+\varepsilon\right)}}{\sqrt{\left(1+\varepsilon\right)\left(J_2+\varepsilon\right)} - \varepsilon\left(J_2-1\right)} \right]^{\frac{2\gamma}{\gamma-1}} \tag{5}$$

Through the relations (1-4), equation (5) determines also the values $u_1=u_2$, a_1 and a_2. The dependencies $J_1(I)$ and $J_2(I)$ of the strengths of waves resulting in pressure discontinuity disintegration on the intensity I of this discontinuity are given by curves 1 and 2 in Fig. 2 (all calculations are performed at $\gamma=1.4$).

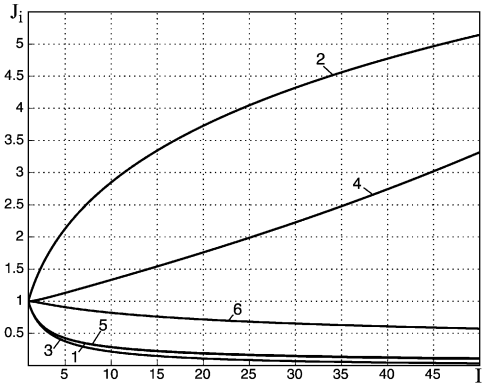

Fig. 2. The dependencies J1(I) and J2(I) of the strengths of waves resulting in pressure discontinuity disintegration on the intensity I of this discontinuity.

Similar conditions of equality of pressures and velocities at the discontinuity K_2 connect the intensities of the Riemann waves r_3, r_4 and r_5:

$$J_3 J_4 = J_5, \qquad [u]_3 + [u]_4 = [u]_5. \tag{6}$$

The strengths of the waves r_1 and r_3 are related by the condition of non-penetration at the left end of the shock tube:

$$[u]_1 + [u]_3 = 0 \tag{7}$$

3 Optimal ratios of linear dimensions

The target under test (mounted at the right end of the shock tube) is affected by a system consisting of the shock wave front s_2 and the rarefaction wave r_5. The gas pressure in the whole region 2 between waves s_2 and r_5 is constant. As the wave s_2 collides with the right end before the start of its interaction with wave r_5 (i.e., to point D), the surface under test is exposed to a wave with a significant section E_1E_2 of constant pressure (Fig. 1c). Such a constant pressure region does not occur in simulated blast waves and, therefore, its generation is a disadvantage of the experiment. On the contrary, if wave s_2 reaches the obstacle at time t_D or after it, its pressure profile (Fig. 1d) is close to the simulated profile of the blast wave. The shock wave s_2 interacts with the refracted rarefaction wave r_5 before its collision with the target end, if only the high-pressure chamber has a certain minimum possible length ($L_2=x_D-x_0$) compared to the length of the low-pressure chamber ($L_1=x_0-x_A$). The minimum permissible ratio $L=L_2/L_1$ depends on the initial pressure ratio I. It can be determined from an analysis of the properties of the resulting waves and discontinuities. The equation $dx/dt=u+a$ of the curvilinear characteristic AB of the wave r_1 is integrated under the conditions of conservation of the Riemann invariant of this wave ($R_+=u+2a/(\gamma-1)$). It helps us to establish how the characteristics of another family with the speed of sound relative to gas particles propagate and lead to their following equation [14, 15]:

$$x - x_0 = \frac{2a(t-t_0)}{\gamma-1} - \frac{x_0 - x_A}{\varepsilon} \cdot \left(\frac{a(t-t_0)}{x_0 - x_A} \right)^{\frac{3-\gamma}{\gamma+1}} \tag{8}$$

In particular, the coordinates of point *B* on the plane of events *(x,t)*

$$x_B = x_0 + \frac{2}{\gamma-1}(x_0 - x_A)\cdot\left(1-\frac{\gamma+1}{2}J_1^{(\gamma-1)/2\gamma}\right)\cdot J_1^{-(\gamma+1)/4\gamma}, \quad (9)$$

$$t_B = t_0 + \frac{x_0 - x_A}{a}\cdot J_1^{-(\gamma+1)/4\gamma} \quad (10)$$

Can be found from equations (2) and (8), which connects the shock wave strength with the change in the sound speed. Conditions (9) and (10), equations of characteristics BC and contact discontinuity *K*

$$(x_C - x_B)/(t_C - t_B) = u_1 + a_1,$$

$$(x_C - x_0)/(t_C - t_0) = u_1$$

Allow us to find the position of point *C* on the contact discontinuity, expressing it in terms of the strength of the primary shock wave r_1 and the length of the high-pressure chamber:

$$x_C - x_0 = \frac{4}{\gamma-1}(x_0 - x_A)\frac{1-J_1^{(\gamma-1)/2\gamma}}{J_1^{(\gamma+1)/4\gamma}}, \quad (11)$$

$$t_C - t_0 = \frac{2(x_0 - x_A)}{aJ_1^{(\gamma+1)/4\gamma}}. \quad (12)$$

To determine the coordinates of point *D*, conditions (11) and (12), equations of the rectilinear characteristic *CD* and the shock wave front s_1 in the section *OD* are used:

$$(x_D - x_C)/(t_D - t_C) = u_2 + a_2,$$

$$(x_D - x_0)/(t_D - t_0) = a\sqrt{(J_2+\varepsilon)/(1+\varepsilon)},$$

As well as relations (1) and (3), which describe the change in parameters at the shock wave front. It results in the following equations:

$$x_D - x_0 = \frac{2(x_0 - x_A)}{J_1^{(\gamma+1)/4\gamma}}\cdot\frac{\sqrt{J_2(1+\varepsilon J_2)/(1+\varepsilon)}}{\varphi(J_1,J_2) - \sqrt{(J_2+\varepsilon)/(1+\varepsilon)}},$$

$$t_D - t_0 = \frac{2(x_0 - x_A)}{a\cdot J_1^{(\gamma+1)/4\gamma}}\cdot\frac{\sqrt{J_2(1+\varepsilon J_2)/(J_2+\varepsilon)}}{\varphi(J_1,J_2) - \sqrt{(J_2+\varepsilon)/(1+\varepsilon)}},$$

Here

$$\varphi(J_1,J_2) = \frac{2}{\gamma-1}\left(1-J_1^{(\gamma-1)/2\gamma}\right) + \sqrt{\frac{J_2(1+\varepsilon J_2)}{J_2+\varepsilon}},$$

And determines the following minimum ratio between the lengths of the low and high pressure chambers:

$$L = \frac{x_D - x_0}{x_0 - x_A} = 2J_1^{-(\gamma+1)/4\gamma} \cdot \frac{\sqrt{J_2(1+\varepsilon J_2)/(1+\varepsilon)}}{\varphi(J_1, J_2) - \sqrt{(J_2+\varepsilon)/(1+\varepsilon)}} \tag{13}$$

At the higher relation of chamber lengths, the considered shock wave has a profile close to triangular. In (13), the strengths $J_1(I)$, $J_2(I)$ are determined by equation (5). The ratio (13) of the shock tube chamber lengths is shown in Fig. 3.

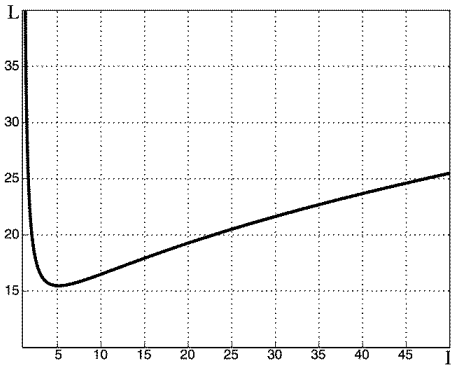

Fig. 3. The ratio of the shock tube chamber lengths.

The minimum relative length of the low pressure chamber (L=15.477) is achieved at I=5.151. At small (I→1) and large (I→∞) initial pressure ratios, low pressure chamber, on the contrary, should be very (theoretically, infinitely) long. The relative length L can be noticeably reduced if a gas with a low molar mass and, therefore, as a high speed of sound a1 is used as a "pushing" substance in the high pressure chamber. The relative length of the low-pressure chamber, described by formula (13), is not only the minimum permissible, but also optimal in the sense that the intensity (J2) and amplitude (Δp) of the leading front of the shock wave acting on the target are easily determined by equation (5). In the case when the collision of wave s2 with an obstacle occurs after the beginning of its interaction with wave r5, its intensity at the moment of collision is somewhat less and is subject to numerical calculation.

4 The degree of pressure decrease in a slipstream

Equations (6) and (7) determine the strengths Ji (i=3..5) of reflected and refracted waves. The solution to equation (7) obtains the wave strengths r1 and r3:

$$J_3 = 1/J_1 \cdot \left(2J_1^{(\gamma-1)/2\gamma} - 1\right)^{2\gamma/(\gamma-1)} \tag{14}$$

The system (6) determines the intensities of the waves r_5 and r_4:

$$J_5 = \left[\frac{a_2 - a_1\left(1 - J_3^{(\gamma-1)/2\gamma}\right)}{a_1 + a_2}\right], \; J_4 = J_5/J_3 \; ;$$

here

$$a_1 = a \cdot J_1^{(\gamma-1)/2\gamma}, \quad a_2 = a\sqrt{J_2\left(1+\varepsilon J_2\right)/\left(J_2+\varepsilon\right)},$$

The intensity J_3 can be determined from the relation (14). Dependences $J_3(I)$, $J_4(I)$, $J_5(I)$ are shown in Fig. 2 (curves 3-5). In the case when the dimensions of the chambers of the shock tube under consideration satisfy relation (13), the pressure drop in a wave with a profile close to triangular incident on the obstacle continues to the value

$$p_5 = J_2 J_5 p_{02}$$

The calculated values of $J_2(I)\cdot J_5(I)$ (curve 6 in Fig. 2) show that the pressure behind the system "shock wave front s_2 and rarefaction wave r_5" drops below the initial (usually atmospheric) pressure p_{02} in the low pressure chamber. Thus, with an optimal choice of the dimensions of the shock tube chambers, not only the positive, but also, partly, the negative phase of the air blast wave, which is characterized by a drop in gas pressure below the atmospheric value, is successfully simulated [16-19].

5 Conclusions

To most fully simulate the high-explosive effect of a blast using shock tubes, the length of the low-pressure chamber in these tubes should significantly exceed the length of the high-pressure one. The minimum acceptable and most convenient ratios of the dimensions of these chambers depend on the initial pressure ratio. Here, they are determined analytically. If those analytically found dimensions are maintained, not only the pressure profile of the first positive phase of the blast wave, which is close to triangular one, is successfully simulated, but also the subsequent pressure drop to a value less than the surrounding pressure, and, consequently, some properties of the negative phase are reproduced.

The study was carried out at the expense of a grant of the Russian Science Foundation No. 22-29-20269, https://rscf.ru/en/project/22-29-20269/, and a grant from the St. Petersburg Science Foundation in accordance with the agreement dated April 15, 2022 No. 57/2022.

References

1. B.E. Gel'fand, S.A. Gubin, S.M. Kogarko, E.I. Timofeev *Passage of shock waves through an interface of two-phase gas-liquid media* Fluid Dynamics, **9**, 914-920. (1974)
2. B.E. Gel'fand, A.V. Gubanov, E.I. Timofeev *Reflection of shock waves by a wall in two-phase gas-bubble-liquid media with variable mass concentration of the gas*. Fluid Dynamics, **17**, 299-302. (1983)
3. A.B. Britan, E.I. Vasil'ev, I.N. Zinovik, I.Yu. Kamynin *Reflection of a blast-profile shock wave from the end wall of the shock tube* Fluid Dynamics, **27**, 412-417 (1992)
4. L.G. Gvozdeva, E.A. Moskvilin, N.B. Scherbak *Interaction of shock waves with porous brittle foams* Proceedings of the 22nd International Symposium on Shock Waves (ISSW22). London, Great Britain, Imperial College, 1999. Southampton, Great Britain: University of Southampton, 1435-1439. (1999)
5. K. Kitagawa, M. Yokoyama *Effect of pressure diffusion of shock wave by porous foam* Proceedings of the 22nd International Symposium on Shock Waves (ISSW22). London, Great Britain, Imperial College, 1999. Southampton, Great Britain: University of Southampton, 1387-1392. (1999)

6. S. Aratani, H. Ojima, G. Jagadeesh, K. Takayama *Fracture in Soda-Lime-Silica Glass Pattern Subjected to Shock Wave Loading* Shock Waves 2001. Proceedings of the Twenty-Third International Symposium on Shock Waves. Arlington, USA: The University of Texas at Arlington, 662-669 (2001)
7. K. Kitagawa, M. Kainuma, H. Ojima, M. Komatsu, K. Takayama, M. Yashihara *Visualization of Shock Wave / Foam Interaction* Shock Waves 2001. Proceedings of the Twenty-Third International Symposium on Shock Waves. Arlington, USA: The University of Texas at Arlington, 603-610. (2001)
8. K. Kitagawa, M. Kainuma, M. Yashuhara *Pressure Attenuation Effect of Shock Wave Passing Through Porous Foam* Shock Waves 2001. Proceedings of the Twenty-Third International Symposium on Shock Waves. Arlington, USA: The University of Texas at Arlington, 596-602. (2001)
9. A. Klomfass, P. Neuwald, K. *Thoma Attenuation of Underwater Shock Waves in Ducts by Air-Filled Wall Panels* Shock Waves 2001. Proceedings of the Twenty-Third International Symposium on Shock Waves. Arlington, USA: The University of Texas at Arlington, 1254-1261. (2001)
10. G. Malamud, D. Levi-Hevroni, A. Levy *Two-dimensional effects of the head on interaction between planar shock wave with low density foam* Shock Waves. Proceedings of the 24th International Symposium on Shock Waves. Beijing, China: Tsinghua University Press and Springer-Verlag, **2**, 1049-1054. (2005)
11. B.W. Skews, S. Bugarin *Shock induced porous barrier flows, with underlying wall pressure amplification* Shock Waves. Proceedings of the 24th International Symposium on Shock Waves. Beijing, China: Tsinghua University Press and Springer-Verlag, **1**, 49-56. (2005)
12. A.N. Polenov, S.M. Frolov, S.A. Tsyganov *Possible applications of shock tubes in studies of explosion processes* Sov. J. Chemical Physics, **5 (1)**, 121-128. (1986)
13. Berezkina M.K., Smirnov I.V., Syshchikova M.P. *The formation of shock waves with an explosive profile in a shock tube* Journal of Applied Mechanics and Technical Physics, **30 (6)**, 879-885. (1989)
14. Uskov V.N. *Traveling One-Dimensional Waves. Part 2* St. Petersburg: Baltic State Technical University "VOENMEH", 188 p. (2013), in Russian
15. K.P. Stanyukovich *Unsteady Motions of a Continuous Medium*, Moscow: Nauka, 856 p. (1971), in Russian
16. M.A. Sadovsky *Selected Works. Geophysics and Physics of Explosion*, Moscow: Nauka, 440 p. (2004), in Russian
17. B.E. Gelfand, M.V. Silnikov *High Explosive Effects of Explosions,* St. Petersburg: Polygon, 272 p. (2002), in Russian
18. B.E. Gelfand, M.V. Silnikov *Chemical and Physical Explosions. Parameters and Control,* St. Petersburg: Polygon, 416 p. (2003), in Russian
19. B.E. Gelfand, M.V. Silnikov *Blast Safety*, St. Petersburg: Asterion, 392 p. (2006), in Russian